Stability analysis of a chain of non-identical vehicles under bilateral cruise control

Wang, Liang and Tisseur, Francoise and Strang, Gilbert and Horn, Berthold K.P.

2019

MIMS EPrint: **2019.3**

ISSN 1749-9097

Stability analysis of a chain of non-identical vehicles under bilateral cruise control

Liang Wang[a], Françoise Tisseur[b], Gilbert Strang[c] and Berthold K.P. Horn[d*]

***Abstract*—Bilateral cruise control (BCC) suppresses traffic flow instabilities. Previously, for simplicity of analysis, vehicles in BCC traffic flow were assumed to be identical, i.e., using the same gains for control. In this study, we analyze the stability of an inhomogeneous vehicular chain in which the gains used by different vehicles are not the same. Not unexpectedly, mathematical analysis becomes more difficult, and leads to a quadratic eigenvalue problem. We study several different cases, and shows that a chain of vehicles under bilateral cruise control is stable even when the vehicles do not all have the same control system properties. Numerical simulations validate the analysis.**

***Index Terms*—bilateral cruise control (BCC), linear feedback control, stability analysis, inhomogeneous system, quadratic eigenvalue problem.**

I. Introduction and related work

FOR self-driving cars, and those with some form of driver assistance, several measurements of the environment can be obtained simultaneously. For instance, for a sensor based control system, it is no more difficult to "look back" than it is to "look forward." New control strategies should be explored that exploit this increased capability. For instance, it has been shown that "stop-and-go" traffic and "phantom traffic jams" (appearing regularly in today's highway traffic) can be suppressed in traffic flow using newly designed cars with some form of advanced cruise control. One basic question is how to control a chain of cars. Should control be global and central? How much "freedom" should be given to individual cars? Several models have been proposed.

One well-known approach is platoon control [1]–[4]. In brief, the platoon controller tries to "bind" successive cars together and force them to move in lock-step like carriages in a train. In general, a single lead vehicle controls a whole chain and plays the same role as a locomotive in a train. New platoon models, e.g., decentralized platoon, bi-directional platoon, multi-neighbor platoon, are continuing to be proposed [5]–[13]. See also [14], [15] for theoretical analyses of various platoon models. Some questions immediately come to mind, for instance, "are self-driving cars willing to give up their freedom?", "will the passengers in the self-driving cars trust other vehicles and allow very tight spacing between cars?", "who should be the lead vehicle? (why not me?)" and so on.

A different approach is to reserve as much freedom for self-driving cars as for human drivers. Newly designed adaptive cruise control (ACC) systems control vehicles moving independently like cars, rather than like carriages in a train. In this approach, global-control parameters, such as (preset) desired speed and (preset) desired spacing between cars, are *not* allowed. The control system (including control commands such as the desired acceleration) of one car is *not* accessible to ACC systems in other cars. The input of the ACC system comes from the vehicle's on-board sensors, and control of the vehicle is based entirely on the outputs of its own sensors. One newly extended ACC system is known as bilateral cruise control (BCC) [16]–[19], in which the vehicle is controlled to stay as far from the leading car as from the following car. See also [20]–[22] for previous efforts involving use of bi-directional information flow.

This "freedom" also means that vehicles in the traffic flow need *not* be identical. Even if the same control strategy is used, the mass and control ability may be different for different cars. In this paper, we study a line of inhomogeneous traffic flow containing vehicles with different control gains. All vehicles use bilateral cruise control. For stability analysis, control of each vehicle is simplified to a linear feedback system. But, unlike previous analyses, in which all cars are assumed to use the same control gains [5]–[8], [16]–[19], we explore here the more general case in which vehicles preserve their "individuality" by using different gains. The corresponding mathematical analysis becomes more difficult than the case of identical-vehicle flow, and thus, such analysis, and the corresponding results, have *not* been explored before (at least not in the field of ACC design and traffic stability analysis). We study several cases — from special to more and more general. Different from traditional quadratic eigenvalue problem (QEP) corresponding to some physical models, e.g. mechanical structure analysis [23], Newton III will not be assumed when we analyze the QEP corresponding to a chain of non-identical vehicles. As a result, the stability analysis of such non-identical vehicular chain is not trivial. In this paper, we provide some mathematical "tricks" to prove the stability of the non-identical vehicular chain under BCC.

The stability analysis of non-identical vehicular chains under BCC shows that bilateral cruise control absolutely does *not* require wireless communication. Only one simple rule is used: aim to stay in the middle. This works even if the control strategy is implemented differently in different vehicles (i.e., using different gains). Such BCC cars can be made

[a] School of Electronics and Communication Engineering, Sun Yat-sen University (SYSU), Guangdong, 510275, China, e-mail: wangliang@csail.mit.edu
[b] School of Mathematics, University of Manchester, Manchester M13 9PL, UK, e-mail: francoise.tisseur@manchester.ac.uk. Supported by a Royal Society-Wolfson Research Merit Award.
[c] Department of Mathematics, MIT, Cambridge, MA 02139, USA, e-mail: gilstrang@gmail.com
[d] Department of Electrical Engineering and Computer Science, MIT, Cambridge, MA 02139, USA, e-mail: bkph@csail.mit.edu
* The corresponding author is Berthold K.P. Horn. This work is sponsored by Toyota Research Institute (TRI) under grant LP-C000765-SR.

differently and run independently. The philosophy of vehicles, namely "control of my car, by my car and for my car", is totally preserved by bilateral cruise control. We also provide numerical simulations to validate the theoretical analysis.

II. Bilateral cruise control review

Let $y_n(t)$ be the position of the nth car, and $v_n(t) = \dot{y}_n(t)$ be its velocity[1]. The pair $\{y_n(t), v_n(t)\}$ gives the state of car n, which is adjusted through the acceleration $a_n(t) = \ddot{y}_n(t)$ commanded by the control system.

In this paper, control of car n is provided by a simple linear feedback system:

$$a_n = k_d(d_n - s_n) + k_v(r_n - u_n), \tag{1}$$

where $d_n = y_{n-1} - y_n - \ell$ denotes the space between the current car and its leading car (with car length ℓ), and $r_n = v_{n-1} - v_n$ denotes the relative velocity between the current car and its leading car. The proportional gain k_d and derivative gain k_v are both *positive*. The desired space s_n and desired speed difference u_n are specified differently in different vehicle-control models as explained next.

For instance, drivers can implement a "constant headway" car-following model (CFM):

$$s_n = s \qquad \text{and} \qquad u_n = 0. \tag{2}$$

Here car n tries to keep a constant space from its leading car $n-1$. Alternatively, the desired space can also be set adaptively by appealing to a constant *reaction time* T. Then

$$s_n = v_n T \qquad \text{and} \qquad u_n = 0. \tag{3}$$

This model is known as "constant-time headway" CFM [24]–[26]. In these two models, control of car n is based *only* on the relative state of car $n-1$ immediately ahead.

For human drivers, it is difficult (or distracting) to look forward and backward simultaneously, however, that is not a problem for a sensor-based control system. A second pair of sensors can be used to measure space and speed difference between the current car and the car following. These two new measurements d_{n+1} and r_{n+1} can then be used for control. For instance, we can set

$$s_n = d_{n+1} \qquad \text{and} \qquad u_n = r_{n+1}. \tag{4}$$

Then, eq. (1) becomes

$$a_n = k_d\big(d_n - d_{n+1}\big) + k_v\big(r_n - r_{n+1}\big). \tag{5}$$

We call this new control strategy the bilateral cruise control (BCC). Here, control of car n is based on the relative positions and relative velocities of *both* car $n-1$ ahead and car $n+1$ behind. The control objective of BCC is to stay in the middle between the "front and back" neighbors, and to run at the average speed of these two neighbors. Fig. 1 shows the car-following control model and bilateral control model. See [16], [17] for more details about implementation of BCC.

[1] Note that y_{n-1} and y_n denote the position of the leading and current cars. The positive direction is chosen as the direction in which cars are moving, thus, $y_{n-1} - y_n > 0$ (see Fig. 1).

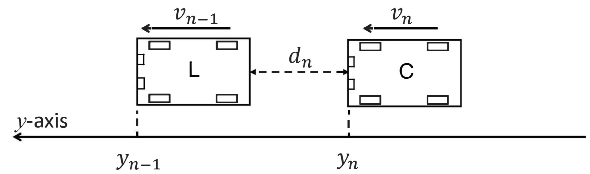

(a) Car-following model

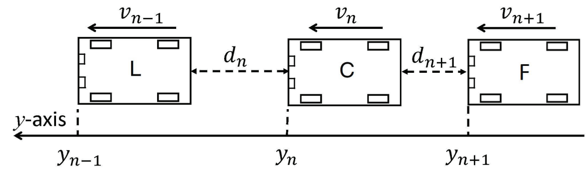

(b) Bilateral cruise control model

Fig. 1. The car-following model (CFM) and bilateral cruise control (BCC) model. The blocks with "L", "C" and "F" denote the leading car, current car and following car. (a) CFM is based *only* on the state of the leading car "L". (b) BCC uses the states of *both* leading car "L" and following car "F".

A physical analog of a line of traffic under BCC is a big "spring-damper-mass" system shown in Fig. 2. Intuitively, a perturbation will lead to damped waves travelling outward in *both* directions from the point of perturbation, and the amplitude of these waves will decay as they travel [17]. Thus, traffic flow under BCC *is* stable for all $k_d > 0$ and $k_v > 0$ [16]–[18]. Ref. [18] provides the analysis of BCC traffic flow under various boundary conditions[2]: infinite line, circular boundaries, fixed-fixed boundaries, free-free boundaries and fixed-free boundaries. Thus, traffic flow instabilities can be suppressed by automated control systems in individual vehicles *without* global control.

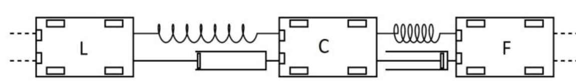

Fig. 2. A physical analog of the traffic flow under bilateral control is a big "spring-damper-mass" system.

Looking at Fig. 2, we can see that *Newton III* applies to two successive masses. That is, the force on the two ends of the "spring" (and similarly the force on the two ends of the "damper") between successive masses are equal in magnitude, and opposite in direction. Actually, Newton III — action equals reaction — can be thought as a special kind of communication: "no matter what I do to you, you do the same to me." In the original BCC model (5), the need for explicit communication between vehicles to enforce this rule is avoided simply by using the same gains k_d and k_v for all vehicles. In effect, in order to guarantee Newton III (and the resulting system stability), vehicles need to be identical in control properties (i.e., having the same gains $\{k_d, k_v\}$). When different gains k_d and k_v are used by different vehicles, Newton III will no longer hold. There will be no physical

[2] The boundaries in platooning are used to control the desired states of all vehicles in the platoon. The boundary condition in BCC is just to design the ACC system such that the car can operate when there is no vehicle ahead and/or no vehicle behind.

analog such as that shown in Fig. 2. The basic question then is "will inhomogeneous traffic flow be stable?" In the rest of this paper, we will study this problem step by step.

III. A LINE OF INHOMOGENEOUS TRAFFIC

We still assume that all vehicles (except the first and last cars) in the traffic flow implement BCC strategy: trying to stay in the middle. The first car 0 (whose leading car is far away) is moving freely at some constant speed $v_0(t) = V$, and the last car N (whose following car is far away) simply implements "constant headway" CFM with $s_N = s$. Now, the vehicles are non-identical, and the attributes, e.g. mass and control ability, for different cars might be different. Mathematically, various gains might be used in different cars. That is, eq. (5) becomes

$$a_n = k_d^{(n)}\big(d_n - d_{n+1}\big) + k_v^{(n)}\big(r_n - r_{n+1}\big) \tag{6}$$

for $n = 1, 2, \cdots, N-1$, and for $n = N$, we find:

$$a_N = k_d^{(N)}\big(d_N - s\big) + k_v^{(N)}\big(r_N - 0\big). \tag{7}$$

Let $x_n(t) = y_n(t) + n\cdot(s+\ell) - y_0(0) - V\cdot t$ be the deviation from the corresponding "equilibrium position" $y_0(0) + V\cdot t - n\cdot(s+\ell)$ where car n was supposed to be, then we find $x_0(t) = 0$, $d_n = x_{n-1} - x_n + s$, $r_n = \dot{x}_{n-1} - \dot{x}_n$ and $a_n = \ddot{x}_n$. Let

$$\mathbf{x}(t) = \big(x_1(t)\ \cdots\ x_n(t)\ \cdots\ x_N(t)\big)^T, \tag{8}$$

then the ordinary differential equation (ODE) system (6) and (7) can be written in the following matrix-vector form:

$$\ddot{\mathbf{x}}(t) + \mathbf{K}_v\mathbf{S}\dot{\mathbf{x}}(t) + \mathbf{K}_d\mathbf{S}\mathbf{x}(t) = \mathbf{0}. \tag{9}$$

Both $\mathbf{K}_d$ and $\mathbf{K}_v$ are (positive) diagonal matrices, i.e.,

$$\mathbf{K}_d = \begin{bmatrix} k_d^{(1)} & & \\ & \ddots & \\ & & k_d^{(N)} \end{bmatrix}, \mathbf{K}_v = \begin{bmatrix} k_v^{(1)} & & \\ & \ddots & \\ & & k_v^{(N)} \end{bmatrix}. \tag{10}$$

The matrix $\mathbf{S}$ is symmetric and positive-definite [27]:

$$\mathbf{S} = \begin{bmatrix} 2 & -1 & & \\ -1 & \ddots & \ddots & \\ & \ddots & 2 & -1 \\ & & -1 & 1 \end{bmatrix}. \tag{11}$$

Actually, $\mathbf{S} = \mathbf{A}^T\mathbf{A}$ with the invertible matrix $\mathbf{A}$ as [28]:

$$\mathbf{A} = \begin{bmatrix} 1 & & & \\ -1 & 1 & & \\ & \ddots & \ddots & \\ & & -1 & 1 \end{bmatrix}. \tag{12}$$

The stability of the non-identical vehicular chain (under BCC) can be studied by eigenvalue analysis.

IV. STABILITY ANALYSIS

The second-order differential equation (9) can be rewritten as a first order differential equation of the twice the dimension,

$$\dot{\mathbf{z}}(t) = \mathbf{C}\mathbf{z}(t), \tag{13}$$

where

$$\mathbf{z}(t) = \begin{bmatrix} \mathbf{x}(t) \\ \dot{\mathbf{x}}(t) \end{bmatrix}, \quad \mathbf{C} = \begin{bmatrix} \mathbf{0} & \mathbf{I} \\ \mathbf{K}_d\mathbf{S} & \mathbf{K}_v\mathbf{S} \end{bmatrix}, \tag{14}$$

with $\mathbf{0}$ the *zero matrix* and $\mathbf{I}$ the *identity matrix*. Then for all finite t, $\mathbf{z}(t) = e^{\mathbf{C}t}\mathbf{b}$ is the unique solution vector of (13) with the initial condition $\mathbf{z}(0) = \mathbf{b}$ [29, Chap. 6]. Hence, the general solution to the differential equation system (9) is given by

$$\mathbf{x}(t) = \begin{bmatrix} \mathbf{I} & \mathbf{0} \end{bmatrix} \mathbf{z}(t) = \begin{bmatrix} \mathbf{I} & \mathbf{0} \end{bmatrix} e^{\mathbf{C}t}\mathbf{b}. \tag{15}$$

The $2N \times 2N$ matrix $\mathbf{C}$ in (14) is called the *companion form* of the $N \times N$ monic quadratic matrix polynomial

$$\mathbf{Q}(\lambda) = \lambda^2\mathbf{I} + \lambda\mathbf{K}_v\mathbf{S} + \mathbf{K}_d\mathbf{S}. \tag{16}$$

The latter has $2N$ finite eigenvalues, counting multiplicities: these are the roots of characteristic polynomial

$$\det\big(\mathbf{Q}(\lambda)\big) = 0,$$

that is, the points $\lambda \in \mathbb{C}$ for which $\mathbf{Q}(\lambda)$ is singular. It is shown in [30], [23] that $\det\big(\mathbf{Q}(\lambda)\big) = \det(\mathbf{C} - \lambda\mathbf{I})$, so $\mathbf{Q}(\lambda)$ and $\mathbf{C}$ share the same eigenvalues [23]. They also have the same Jordan structure. In particular, if

$$\mathbf{C} = \mathbf{Y}\mathbf{J}\mathbf{Y}^{-1} \tag{17}$$

is the Jordan canonical decomposition of $\mathbf{C}$ then $\mathbf{Y}$ has the form

$$\mathbf{Y} = \begin{bmatrix} \mathbf{V} \\ \mathbf{V}\mathbf{J} \end{bmatrix}$$

and (17) is equivalent to

$$\mathbf{V}\mathbf{J}^2 + \mathbf{K}_v\mathbf{S}\mathbf{V}\mathbf{J} + \mathbf{K}_d\mathbf{S}\mathbf{V} = 0, \quad \det\left(\begin{bmatrix} \mathbf{V} \\ \mathbf{V}\mathbf{J} \end{bmatrix}\right) \neq 0. \tag{18}$$

The pair $(\mathbf{V}, \mathbf{J})$ is called a *Jordan pair* for $\mathbf{Q}(\lambda)$. Since $e^{\mathbf{C}t} = \mathbf{Y}e^{\mathbf{J}t}\mathbf{Y}^{-1}$, $\mathbf{x}(t)$ in (15) can be rewritten as

$$\mathbf{x}(t) = \mathbf{V}e^{\mathbf{J}t}\mathbf{c}, \tag{19}$$

where $\mathbf{c} = \mathbf{Y}^{-1}\mathbf{b}$. Now from the explicit expression for the exponential of a Jordan form provided in Appendix B, we find that the solution $\mathbf{x}(t)$ in (20) can be written in the form

$$\mathbf{x}(t) = \sum_{n=1}^{2N} p_n(t)e^{\lambda_n t}\mathbf{v}_n, \tag{20}$$

where the λ_n are the eigenvalues of $\mathbf{Q}(\lambda)$ and the $p_n(t)$ are scalar polynomials in t of bounded degrees. It is then clear that $\mathbf{x}(t)$ decreases exponentially to zero as t tends to infinity if and only if all the eigenvalues λ_n, $n = 1, \ldots, 2N$, have negative real part.

In what follows, we study the stability of the second-order differential equation (9) through the eigenvalues of the associated quadratic matrix polynomial $\mathbf{Q}(\lambda)$ in (16). We proceed step by step: from the most special case to more and more general cases. We repeatedly use the fact that strict equivalence transformations applied to $\mathbf{Q}(\lambda)$ preserve its eigenvalues. Indeed, the quadratic matrix polynomials $\mathbf{Q}(\lambda)$ and $E\mathbf{Q}(\lambda)F$ with E, F nonsingular, have the same eigenvalues since $\det\big(E\mathbf{Q}(\lambda)F\big) = \alpha \det\big(\mathbf{Q}(\lambda)\big)$ where $\alpha = \det(E)\det(F)$ is a nonzero constant. Hence the characteristic polynomials $\det\big(E\mathbf{Q}(\lambda)F\big)$ and $\det\big(\mathbf{Q}(\lambda)\big)$ differ by a nonzero constant and so their roots are equal.

A. Special case: homogeneous traffic

First, let us consider the most special case: homogeneous traffic, in which the gains $k_d^{(n)} = k_d$ and $k_v^{(n)} = k_v$ are the same for all vehicles. As a result, $\mathbf{K}_d = k_d\mathbf{I}$ and $\mathbf{K}_v = k_v\mathbf{I}$, and $\mathbf{Q}(\lambda)$ in (16) becomes

$$\mathbf{Q}(\lambda) = \lambda^2\mathbf{I} + \lambda k_v \mathbf{S} + k_d\mathbf{S}. \tag{21}$$

Since $\mathbf{S}$ is symmetric then, by the spectral theorem [27], there exist $\mathbf{U}$ orthogonal and $\mathbf{D}_\mu$ diagonal such that

$$\mathbf{U}^T\mathbf{S}\mathbf{U} = \mathbf{D}_\mu = \begin{bmatrix} \mu_1 & & \\ & \ddots & \\ & & \mu_N \end{bmatrix}. \tag{22}$$

Here μ_n is an eigenvalue of $\mathbf{S}$ and the nth column of $\mathbf{U}$ is a corresponding eigenvector. Also, since $\mathbf{S}$ is positive definite,

$$\mu_n > 0, \quad n = 1, \dots, N.$$

An explicit expression for μ_n and for the entries of $\mathbf{U}$ is provided in Appendix A. On using (22), we find that the quadratic matrix polynomial

$$\mathbf{U}^T\mathbf{Q}(\lambda)\mathbf{U} = \lambda^2\mathbf{I} + \lambda k_v\mathbf{D}_\mu + k_d\mathbf{D}_\mu$$

is diagonal and

$$\det\big(\mathbf{Q}(\lambda)\big) = \det\big(\mathbf{U}^T\mathbf{Q}(\lambda)\mathbf{U}\big) = \prod_{n=1}^{N}(\lambda^2 + \lambda k_v\mu_n + k_d\mu_n).$$

As a result, the $2N$ eigenvalues of $\mathbf{Q}(\lambda)$ can be expressed in terms of the N eigenvalues μ_n of $\mathbf{S}$ as

$$\lambda_{2n-1} = \frac{-k_v\mu_n + \sqrt{k_v^2\mu_n^2 - 4k_d\mu_n}}{2}, \tag{23}$$

$$\lambda_{2n} = \frac{-k_v\mu_n - \sqrt{k_v^2\mu_n^2 - 4k_d\mu_n}}{2}, \tag{24}$$

$n = 1, \dots, N$. Since $\mu_n > 0$, $k_d > 0$ and $k_v > 0$, all the eigenvalues of $\mathbf{Q}(\lambda)$ have negative real part. In summary, we proved the following result.

Theorem IV.1. *The system*

$$\ddot{\mathbf{x}}(t) + k_v\mathbf{S}\dot{\mathbf{x}}(t) + k_d\mathbf{S}\mathbf{x}(t) = \mathbf{0} \tag{25}$$

corresponding to homogeneous traffic is stable.

It turns out that the solution $\mathbf{x}(t)$ to (25) can be written explicitly in terms of the eigenvalues and eigenvectors of $\mathbf{S}$. Indeed, the columns of $\mathbf{U} = [\mathbf{u}_1, \dots, \mathbf{u}_N]$ are eigenvectors of $\mathbf{S}$ but they are also eigenvectors of $\mathbf{Q}(\lambda)$. In particular, $\mathbf{u}_n$ is an eigenvector of $\mathbf{Q}(\lambda)$ with eigenvalues λ_{2n-1} and λ_{2n}, i.e.,

$$\mathbf{Q}(\lambda_{2n-1})\mathbf{v}_n = 0, \quad \mathbf{Q}(\lambda_{2n})\mathbf{v}_n = 0.$$

Also, the Jordan form of diagonalizable quadratic matrix polynomials can only have 1×1 and 2×2 blocks [31, Sec. 3], the latter arising when scalar quadratics on the diagonal of the diagonalized quadratic matrix polynomial have two equal roots.

It is easy to check that with $\Lambda = \mathrm{diag}(\lambda_1, \lambda_2, \dots, \lambda_{2N})$ and $\mathbf{e}_n$ denoting the nth column of the $2N \times 2N$ identity matrix, the pair $(\mathbf{V}, \mathbf{J})$ where

$$\mathbf{V} = \begin{bmatrix} \mathbf{u}_1 & \mathbf{u}_1 & \mathbf{u}_2 & \mathbf{u}_2 & \dots & \mathbf{u}_N & \mathbf{u}_N \end{bmatrix}, \tag{26}$$

$$\mathbf{J} = \begin{cases} \Lambda & \text{if } \mu_n \neq 4k_d/k_v^2 \text{ for all } n, \\ \Lambda + \mathbf{e}_{2j-1}\mathbf{e}_{2j}^T & \text{if } \mu_j = 4k_d/k_v^2 \text{ for some } j, \end{cases} \tag{27}$$

forms a Jordan pair for $\mathbf{Q}(\lambda)$, that is, $(\mathbf{V}, \mathbf{J})$ satisfies (18) with $\mathbf{K}_d = k_d\mathbf{I}$ and $\mathbf{K}_v = k_v\mathbf{I}$. In other words, for our specific quadratic matrix polynomial, the Jordan matrix is diagonal unless there is a j such that $\mu_j = 4k_d/k_v^2$, in which case the eigenvalue $\lambda_{2j-1} = \lambda_{2j}$ belongs to a 2×2 Jordan block. Hence, it follows from (19) that when $\mu_n \neq 4k_d/k_v^2$ for all n then

$$\mathbf{x}(t) = \sum_{n=1}^{N}(c_{2n-1}e^{\lambda_{2n-1}t} + c_{2n}e^{\lambda_{2n}t})\mathbf{u}_n, \tag{28}$$

and when there exists j such that $\mu_j = 4k_d/k_v^2$ then

$$\mathbf{x}(t) = \sum_{n=1}^{N}(c_{2n-1}e^{\lambda_{2n-1}t} + c_{2n}e^{\lambda_{2n}t})\mathbf{u}_n + c_{2j}te^{\lambda_{2j}t}\mathbf{u}_j, \tag{29}$$

where c_n, $n = 1, \dots, 2N$, are constants determined by the initial conditions. Since the eigenvalues and eigenvectors of $\mathbf{S}$ are known explicitly–see appendix A, the $2N$ eigenvalues λ_j of $\mathbf{Q}(\lambda)$ in (23)–(24) are also known explicitly and hence $\mathbf{x}(t)$ in (28) or (29) provides and explicit expression for the solution to the second-order system in (25).

B. More general case: proportional and derivative gains with constant ratio

Second, let us consider a more general case: the proportional gains $k_d^{(n)}$ and the derivative gains $k_v^{(n)}$ are different for different vehicles, but, their ratio is constant, i.e., $k_v^{(n)} = \tau k_d^{(n)}$ for all n (with $\tau > 0$). Then (16) becomes

$$\mathbf{Q}(\lambda) = \lambda^2\mathbf{I} + \lambda\tau\mathbf{K}_d\mathbf{S} + \mathbf{K}_d\mathbf{S}. \tag{30}$$

Since the diagonal matrix $\mathbf{K}_d$ has positive diagonal entries,

$$\mathbf{K}_d^{1/2} = \begin{bmatrix} \sqrt{k_d^{(1)}} & & \\ & \ddots & \\ & & \sqrt{k_d^{(N)}} \end{bmatrix} \tag{31}$$

is nonsingular and since $\mathbf{S}$ is symmetric positive definite, so is $\mathbf{K}_d^{1/2}\mathbf{S}\mathbf{K}_d^{1/2}$. Hence, as in the special case of homogeneous traffic described in section IV-A, there exist an orthogonal matrix $\mathbf{U} = [\mathbf{u}_1, \ldots, \mathbf{u}_N]$ and a diagonal matrix $\mathbf{D}_\mu = \mathrm{diag}(\mu_1, \ldots, \mu_N)$ with positive diagonal entries such that

$$\mathbf{U}^T(\mathbf{K}_d^{1/2}\mathbf{S}\mathbf{K}_d^{1/2})\mathbf{U} = \mathbf{D}_\mu. \tag{32}$$

But unlike for the matrix $\mathbf{S}$, we do not have an explicit expression for the eigenpairs of $\mathbf{K}_d^{1/2}\mathbf{S}\mathbf{K}_d^{1/2}$. Nevertheless the quadratic matrix polynomial $\mathbf{Q}(\lambda)$ in (30) can be diagonalized via similarity with $\mathbf{T} = \mathbf{K}_d^{1/2}\mathbf{U}$. Indeed, on using (32) and the orthogonality of $\mathbf{U}$, we find that $\mathbf{Q}(\lambda)$ is similar to the diagonal quadratic matrix polynomial

$$\begin{aligned}\mathbf{T}^{-1}\mathbf{Q}(\lambda)\mathbf{T} &= \mathbf{U}^T\mathbf{K}_d^{-1/2}\mathbf{Q}(\lambda)\mathbf{K}_d^{1/2}\mathbf{U}\\ &= \lambda^2\mathbf{I} + \lambda\tau\mathbf{D}_\mu + \mathbf{D}_\mu,\end{aligned}$$

whose $2N$ eigenvalues (and thereby that of $\mathbf{Q}(\lambda)$) are given by (for $n = 1, \ldots, N$)

$$\lambda_{2n-1} = (-\tau\mu_n + \sqrt{\tau^2\mu_n^2 - 4\mu_n})/2, \tag{33}$$
$$\lambda_{2n} = (-\tau\mu_n - \sqrt{\tau^2\mu_n^2 - 4\mu_n})/2, \tag{34}$$

Since $\mu_n > 0$ for all n and $\tau > 0$, the eigenvalues of $\mathbf{Q}(\lambda)$ all have negative real part. This leads to the following result.

Theorem IV.2. *The system*

$$\ddot{\mathbf{x}}(t) + \tau\mathbf{K}_d\mathbf{S}\dot{\mathbf{x}}(t) + \mathbf{K}_d\mathbf{S}\mathbf{x}(t) = \mathbf{0} \tag{35}$$

corresponding to the case of constant ratio between the proportional gains and the derivative gains is stable.

If we let

$$\mathcal{N} = \{n : \mu_n = 4/\tau^2\}$$

then for $\mathbf{V}$ and $\mathbf{J}$ in (19) we have

$$\begin{aligned}\mathbf{V} &= \mathbf{K}_d^{1/2}\begin{bmatrix}\mathbf{u}_1 & \mathbf{u}_1 & \mathbf{u}_2 & \mathbf{u}_2 & \ldots & \mathbf{u}_N & \mathbf{u}_N\end{bmatrix},\\ \mathbf{J} &= \mathrm{diag}(\lambda_1, \lambda_2, \ldots, \lambda_{2N}) + \sum_{n\in\mathcal{N}} \mathbf{e}_{2n-1}\mathbf{e}_{2n}^T.\end{aligned}$$

Hence there are 2×2 Jordan blocks when $\mathcal{N}$ is not the emptyset. It then follows from (19) that

$$\begin{aligned}\mathbf{x}(t) &= \sum_{n=1}^{N}(c_{2n-1}e^{\lambda_{2n-1}t} + c_{2n}e^{\lambda_{2n}t})\mathbf{K}_d^{1/2}\mathbf{u}_n\\ &\quad + \sum_{n\in\mathcal{N}} c_{2n}te^{\lambda_{2n}t}\mathbf{K}_d^{1/2}\mathbf{u}_n,\end{aligned}$$

where c_n, $n = 1, \ldots, 2N$ are constants determined by the initial conditions.

C. The most general case

Now, let us consider the most general case of (16), in which $\mathbf{K}_d$ and $\mathbf{K}_v$ are two different positive diagonal matrices (not just multiples of one another). Since $\mathbf{S}$ is symmetric positive definite, it has a unique symmetric positive definite square root, which we denote by $\mathbf{S}^{1/2}$ [32, Cor. 1.30]. It follows from (22) that

$$\mathbf{S}^{1/2} = \mathbf{U}\begin{bmatrix}\sqrt{\mu_1} & & \\ & \ddots & \\ & & \sqrt{\mu_N}\end{bmatrix}\mathbf{U}^T$$

since $\mathbf{S}^{1/2}\mathbf{S}^{1/2} = \mathbf{S}$, $\mathbf{S}^{1/2}$ is symmetric and it is positive definite since all its eigenvalues are positive. It then follows that $\mathbf{S}^{1/2}$ is nonsingular. On using $\mathbf{S}^{1/2}$, we find that $\mathbf{Q}(\lambda)$ is similar to the symmetric quadratic matrix polynomial

$$\begin{aligned}\widetilde{\mathbf{Q}}(\lambda) &:= \mathbf{S}^{1/2}\mathbf{Q}(\lambda)\mathbf{S}^{-1/2}\\ &= \lambda^2\mathbf{I} + \lambda\mathbf{S}^{1/2}\mathbf{K}_v\mathbf{S}^{1/2} + \mathbf{S}^{1/2}\mathbf{K}_d\mathbf{S}^{1/2}.\end{aligned} \tag{36}$$

But since $\mathbf{S}^{1/2}\mathbf{K}_v\mathbf{S}^{1/2}$ and $\mathbf{S}^{1/2}\mathbf{K}_d\mathbf{S}^{1/2}$ do not commute when $\mathbf{K}_d \neq \mathbf{K}_v$, $\widetilde{\mathbf{Q}}(\lambda)$ cannot be reduced further to diagonal form by congruence transformation [33].

Letting $\mathbf{w} = \mathbf{S}^{1/2}\mathbf{u}$, we have that $\mathbf{S}^{1/2}\mathbf{u} = 0$ if and only if $\mathbf{u} = 0$ since $\mathbf{S}^{1/2}$ is nonsingular. Hence, for $s = v$ and $s = d$, and for all nonzero vectors $\mathbf{u} \in \mathbb{C}^N$,

$$\mathbf{u}^*\big(\mathbf{S}^{1/2}\mathbf{K}_s\mathbf{S}^{1/2}\big)\mathbf{u} = \mathbf{w}^*\mathbf{K}_s\mathbf{w} = \sum_{n=1}^{N} k_v^{(n)}|w_n|^2 > 0, \tag{37}$$

where $\mathbf{u}^* = \overline{\mathbf{u}}^T$ denotes the conjugate transpose of $\mathbf{u}$. This shows that the symmetric matrices $\mathbf{S}^{1/2}\mathbf{K}_v\mathbf{S}^{1/2}$ and $\mathbf{S}^{1/2}\mathbf{K}_d\mathbf{S}^{1/2}$ are positive definite.

Let $\mathbf{v}_n \neq \mathbf{0}$ be an eigenvector of $\widetilde{\mathbf{Q}}(\lambda)$ in (36). Then at least one of the two roots of the quadratic scalar polynomial

$$\mathbf{v}_n^*\widetilde{\mathbf{Q}}(\lambda)\mathbf{v}_n = \lambda^2 + c(\mathbf{v}_n)\lambda + k(\mathbf{v}_n) = 0 \tag{38}$$

where

$$\begin{aligned}c(\mathbf{v}_n) &= \mathbf{v}_n^*\big(\mathbf{S}^{1/2}\mathbf{K}_v\mathbf{S}^{1/2}\big)\mathbf{v}_n,\\ k(\mathbf{v}_n) &= \mathbf{v}_n^*\big(\mathbf{S}^{1/2}\mathbf{K}_d\mathbf{S}^{1/2}\big)\mathbf{v}_n\end{aligned}$$

is an eigenvalue of $\widetilde{\mathbf{Q}}(\lambda)$ with eigenvector $\mathbf{v}_n$. But by (37), $c(\mathbf{v}_n) > 0$ and $k(\mathbf{v}_n) > 0$ since $\mathbf{v}_n \neq \mathbf{0}$, and hence the roots of the quadratic polynomial in (38) have negative real part. This implies that the eigenvalue of $\widetilde{\mathbf{Q}}(\lambda)$ with eigenvector $\mathbf{v}_n$ has negative real part. Since this result holds for all the eigenvectors $\mathbf{v}_n$ of $\widetilde{\mathbf{Q}}(\lambda)$, $n = 1, \ldots, 2N$, all the eigenvalues of $\widetilde{\mathbf{Q}}(\lambda)$, and therefore those of $\mathbf{Q}(\lambda)$, have negative real part. We have proven the following theorem.

Theorem IV.3. *The BCC traffic flow of non-identical vehicles described by the ODE* (9) *is* stable.

Thus, the solution $\mathbf{x}(t)$ to (9) will be close to zero when t is large, or equivalently

$$y_n(t) \to y_0(0) + Vt - n(s + \ell), \quad n = 1, \ldots, N,$$

that is, from arbitrary initial state, the inhomogeneous BCC traffic will go to the *equilibrium state* in which all vehicles are equally spaced by s and move at the same speed V.

In summary, smart driving is pretty simple, just try to stay in the middle! This is the basic rule (which stops tailgating) used in BCC. Vehicles can implement the basic rule independently and differently. The traffic flow system will still be stable (Theorem IV.3), and thus, smooth traffic flow can be achieved *without* the need for communication between vehicles (V2V) or between vehicles and the infrastructure (V2R).

V. Simulation

We built a simulator to verify the theoretical analysis. Fig. 3 show simulation results (when $N = 32$). See [35] for the video and MATLAB code (numerical implementation of (6)). The time step is $\Delta t = 0.1$ sec. Speed limits are 0 and 160 km/h (or 44.44 m/sec.), and acceleration/deceleration limits are 5 and -5 m/sec^2. In the simulation of Fig. 3, vehicles of two types are mixed randomly. For the first type of (totally 16) vehicle (black curves and red squares in Fig. 3), relatively large proportional gain is used: $k_d^{(n)}$ is chosen as a random number between 0.2 to 0.4 1/sec^2, and the derivative gain $k_v^{(n)}$ is chosen as a random number between 0.05 to 0.15 1/sec. For the second type of (totally 16) cars (red curves and red squares in Fig. 3), relatively small proportional gain is used: $k_d^{(n)}$ is chosen as a random number between 0.05 to 0.15 1/sec^2, and the derivative gain $k_v^{(n)}$ is chosen as a random number between 0.2 to 0.4 1/sec. Initially, the space between cars is set as a random number between 5 to 45 meters, and the speed is randomly chosen from 20 to 30 m/sec. In order to show the simulation results, we let the cars run on a "loop" which is longer than the total length of the traffic flow.

In the first 100 sec., the first car, i.e., the bold curve and solid square in Fig. 3, is moving at the constant speed of 25 m/sec. The stability of BCC traffic (Theorem 3) guarantees that perturbations, i.e., departure from equilibrium state, in the initial condition dissipate (See Fig. 3(b)). At 100 sec, the first car brakes suddenly at -5 m/sec^2 for 2 sec., and then speeds up again at 5 m/sec^2 for another 2 sec. (See the first curve in Fig. 3(a)). Still, due to the system's stability, the induced perturbations are suppressed effectively (See Fig. 3(c)), rather than are amplified to cause "phantom traffic jams" as they would be in today's highway traffic [17].

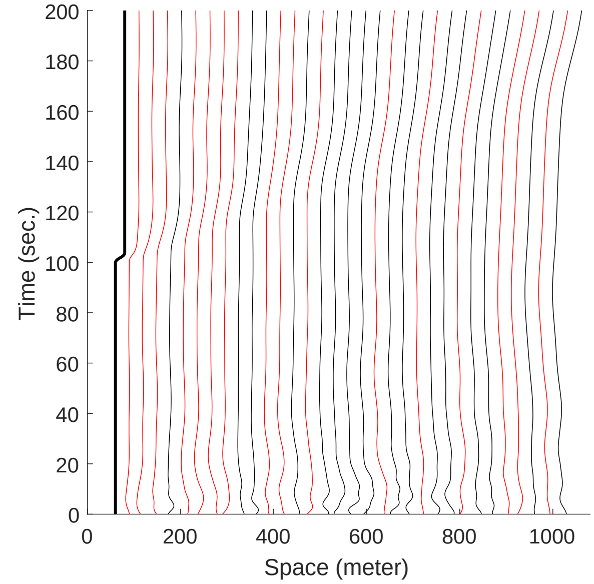

(a) Cars' trajectories in relative reference (25 m/sec.)

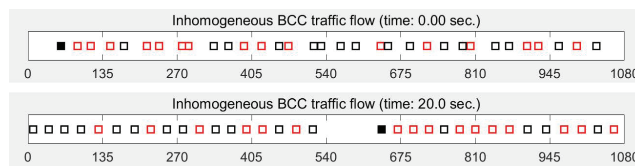

(b) Initial state and traffic flow after 20 sec.

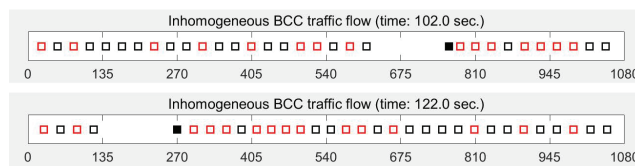

(c) Traffic flow at 102 sec. and 122 sec.

Fig. 3. Simulation results. (a) Trajectories of traffic flow in a relative reference frame which moves at 25 m/sec. Red curves correspond to cars whose $k_d \in (0.05, 0.15)$ and $k_v \in (0.2, 0.4)$ randomly. Black curves correspond to cars whose $k_d \in (0.2, 0.4)$ and $k_v \in (0.05, 0.15)$ randomly. At 100 sec., The first car (bold black curve) brakes hardly for 2 sec. (b) The perturbations in the initial traffic state dissipate due to the stability of BCC. (c) The perturbations due to sudden brake of the first car also dissipate.

VI. Conclusion

In today's traffic, drivers focus mostly on the car ahead, and implement car-following control. This results in traffic flow instabilities, including alternating "stop-and-go" driving conditions. Such traffic flow instabilities can be suppressed effectively if the vehicle also takes into account the state of the car following it. Different from human drivers, ACC system equipped with suitable sensors can implement BCC easily. Thus, we can expect smooth traffic in the future when BCC vehicles are widely used.

Bilateral cruise control guarantees "freedom" of vehicles. Basically, "control of my car is by my car and for my car." In previous work, traffic is assumed to be *homogenous*. That is, the same gains are used in the control systems of all of the vehicles. (This hypothesis is also widely used in the study of platooning models). In the case of BCC, the hypothesis of homogenous traffic, i.e., identical vehicles, guarantees that Newton III applies. However, the mass and control abilities of various vehicles might be different, so that satisfying Newton III would actually require communication. We show here that there is no need for inter-vehicle communication while reaping the benefits of bilateral control. We prove that inhomogeneous traffic is still *stable* under bilateral cruise control (Theorem IV.3). Thus, the new driving strategy — trying to stay in the middle — can be implemented independently by different vehicles, and smooth traffic flow can be guaranteed.

In this paper, we only consider the ideal linear feedback control (which is the simplification of the physical implementation ACC and BCC systems). In real application, delay and non-linearity should also be considered [26]. Moreover, mixed traffic containing human-drivers and BCC vehicles will also be an interesting problem. These are some of the topics for future work.

Appendix A
The eigenpairs of discrete Laplacian

The tri-diagonal symmetric and positive definite matrix $\mathbf{S}$ in (11) is a one dimensional (1-d) discrete Laplacian operator with fixed-free boundaries [28]. Thus, the eigenvalues μ_n of $\mathbf{S}$ are *positive* for all n, and all (unit) eigenvectors $\{\mathbf{u}_n\}$ form an *orthogonal matrix* $\mathbf{U} = \left[\mathbf{u}_1 \ldots \mathbf{u}_n \ldots \mathbf{u}_N\right]$ with $\mathbf{U}^T\mathbf{U} = \mathbf{I}$

[27]. The m-th entry $u_{m,n}$ in the eigenvector $\mathbf{u}_n$ — which is also the entry in row m and column n of $\mathbf{U}$ — is

$$u_{m,n} = \sqrt{\frac{2}{N}} \sin\left(\frac{(2n-1)m}{2N+1}\pi\right), \tag{39}$$

and the corresponding eigenvalue is (pp. 543 in [34]):

$$\mu_n = 2 - 2\cos\left(\frac{2n-1}{2N+1}\pi\right) = 4\sin^2\left(\frac{2n-1}{2N+1}\frac{\pi}{2}\right). \tag{40}$$

Thus, $\mu_n > 0$ for all $n = 1, 2, \cdots, N$.

Appendix B
The exponential of a Jordan matrix

Let $\mathbf{J} = \mathrm{diag}(\mathbf{J}_1, \mathbf{J}_2, \ldots, \mathbf{J}_p)$ be a Jordan matrix, where $\mathbf{J}_i$ is an $m_i \times m_i$ Jordan block with eigenvalue λ_i, that is,

$$\mathbf{J}_k = \begin{bmatrix} \lambda_k & 1 & & \\ & \lambda_k & \ddots & \\ & & \ddots & 1 \\ & & & \lambda_k \end{bmatrix} \in \mathbb{C}^{m_k \times m_k}.$$

Then

$$e^{\mathbf{J}t} = \mathrm{diag}(e^{\mathbf{J}_1 t}, e^{\mathbf{J}_2 t}, \ldots, e^{\mathbf{J}_p t}),$$

where

$$e^{\mathbf{J}_i t} = e^{\lambda_i t} \begin{bmatrix} 1 & t & \frac{t^2}{2!} & \cdots & \frac{t^{(m_i-1)}}{(m_i-1)!} \\ & \ddots & \ddots & \ddots & \vdots \\ & & \ddots & \ddots & \frac{t^2}{2!} \\ & & & \ddots & t \\ & & & & 1 \end{bmatrix}. \tag{41}$$

References

[1] W. Levine and M. Athans, "On the optimal error regulation of a string of moving vehicles," *IEEE Transactions on Automatic Control*, vol. 11, no. 3, pp. 355–361, 1966.

[2] P. Varaiya, "Smart cars on smart roads: problems of control," *IEEE Transactions on automatic control*, vol. 38, no. 2, pp. 195–207, 1993.

[3] D. N. Godbole and J. Lygeros, "Longitudinal control of the lead car of a platoon," *IEEE Transactions on Vehicular Technology*, vol. 43, no. 4, pp. 1125–1135, 1994.

[4] S. S. Stankovic, M. J. Stanojevic, and D. D. Siljak, "Decentralized overlapping control of a platoon of vehicles," *IEEE Transactions on Control Systems Technology*, vol. 8, no. 5, pp. 816–832, 2000.

[5] P. Barooah, P. G. Mehta, and J. P. Hespanha, "Mistuning-based control design to improve closed-loop stability margin of vehicular platoons," *IEEE Trans. on Automatic Control*, vol. 54, no. 9, pp. 2100–2113, 2009.

[6] R. H. Middleton and J. H. Braslavsky, "String instability in classes of linear time invariant formation control with limited communication range," *IEEE Transactions on Automatic Control*, vol. 55, no. 7, pp. 1519–1530, 2010.

[7] F. Lin, M. Fardad, and M. R. Jovanovic, "Optimal control of vehicular formations with nearest neighbor interactions," *IEEE Transactions on Automatic Control*, vol. 57, no. 9, pp. 2203–2218, 2012.

[8] H. Hao, P. Barooah, and P. G. Mehta, "Stability margin scaling laws for distributed formation control as a function of network structure," *IEEE Transactions on Automatic Control*, vol. 56, no. 4, pp. 923–929, 2011.

[9] Y. Zheng, S. E. Li, J. Wang, D. Cao, and K. Li, "Stability and scalability of homogeneous vehicular platoon: Study on the influence of information flow topologies," *IEEE Transactions on Intelligent Transportation Systems*, vol. 17, no. 1, pp. 14–26, 2016.

[10] Y. Zheng, S. E. Li, K. Li, and L.-Y. Wang, "Stability margin improvement of vehicular platoon considering undirected topology and asymmetric control," *IEEE Transactions on Control Systems Technology*, vol. 24, no. 4, pp. 1253–1265, 2016.

[11] S. E. Li, X. Qin, K. Li, J. Wang, and B. Xie, "Robustness analysis and controller synthesis of homogeneous vehicular platoons with bounded parameter uncertainty," *IEEE/ASME Transactions on Mechatronics*, vol. 22, no. 2, pp. 1014–1025, 2017.

[12] Y. Zheng, S. E. Li, K. Li, and W. Ren, "Platooning of connected vehicles with undirected topologies: Robustness analysis and distributed h-infinity controller synthesis," *IEEE Transactions on Intelligent Transportation Systems*, vol. 19, no. 5, pp. 1353–1364, 2018.

[13] H. Hao and P. Barooah, "On achieving size-independent stability margin of vehicular lattice formations with distributed control," *IEEE Transactions on Automatic Control*, vol. 57, no. 10, pp. 2688–2694, 2012.

[14] J. Ploeg, N. Van De Wouw, and H. Nijmeijer, "Lp string stability of cascaded systems: Application to vehicle platooning," *IEEE Transactions on Control Systems Technology*, vol. 22, no. 2, pp. 786–793, 2014.

[15] E. Shaw and J. K. Hedrick, "String stability analysis for heterogeneous vehicle strings," in *American Control Conference, 2007. ACC'07*. IEEE, 2007, pp. 3118–3125.

[16] B. K. Horn, "Suppressing traffic flow instabilities," in *Intelligent Transportation Systems-(ITSC), 2013 16th International IEEE Conference on*. IEEE, 2013, pp. 13–20.

[17] B. K. Horn and L. Wang, "Wave equation of suppressed traffic flow instabilities," *IEEE Transactions on Intelligent Transportation Systems*, vol. 19, no. 9, pp. 2955–2964, 2018.

[18] L. Wang, B. K. Horn, and G. Strang, "Eigenvalue and eigenvector analysis of stability for a line of traffic," *Studies in Applied Mathematics*, vol. 138, no. 1, pp. 103–132, 2017.

[19] T. A. Baran and B. K. Horn, "A robust signal-flow architecture for cooperative vehicle density control." in *ICASSP*, 2013, pp. 2790–2794.

[20] A. Nakayama, Y. Sugiyama, and K. Hasebe, "Effect of looking at the car that follows in an optimal velocity model of traffic flow," *Physical Review E*, vol. 65, no. 1, p. 016112, 2001.

[21] M. Treiber and D. Helbing, "Hamilton-like statistics in onedimensional driven dissipative many-particle systems," *The European Physical Journal B*, vol. 68, no. 4, pp. 607–618, 2009.

[22] P. A. Ioannou and C. C. Chien, "Autonomous intelligent cruise control," *IEEE Trans. on Vehicular technology*, vol. 42, no. 4, pp. 657–672, 1993.

[23] F. Tisseur and K. Meerbergen, "The quadratic eigenvalue problem," *SIAM review*, vol. 43, no. 2, pp. 235–286, 2001.

[24] M. J. Lighthill and G. B. Whitham, "On kinematic waves ii. a theory of traffic flow on long crowded roads," *Proc. R. Soc. Lond. A*, vol. 229, no. 1178, pp. 317–345, 1955.

[25] T. Nagatani, "Traffic jams induced by fluctuation of a leading car," *Physical Review E*, vol. 61, no. 4, p. 3534, 2000.

[26] P. Ioannou and Z. Xu, "Throttle and brake control systems for automatic vehicle following," *IVHS Journal*, vol. 1, no. 4, pp. 345–377, 1994.

[27] G. Strang, *Introduction to linear algebra*. Wellesley-Cambridge Press, 2016.

[28] ——, *Computational science and engineering*. Wellesley-Cambridge Press, 2007.

[29] P. Lancaster, *Lambda-Matrices and Vibrating Systems*. Oxford: Pergamon Press, 1966, reprinted by Dover, New York, 2002.

[30] I. Gohberg, P. Lancaster, and L. Rodman, *Matrix Polynomials*. Philadelphia, PA, USA: Society for Industrial and Applied Mathematics, 2009, unabridged republication of book first published by Academic Press in 1982.

[31] P. Lancaster and I. Zaballa, "Diagonalizable quadratic eigenvalue problems," *Mechanical Systems and Signal Processing*, vol. 23, no. 4, pp. 1134–1144, 2009.

[32] N. J. Higham, *Functions of Matrices: Theory and Computation*. Philadelphia, PA, USA: Society for Industrial and Applied Mathematics, 2008.

[33] T. Caughey and M. O'Kelly, "Classical normal modes in damped linear dynamic systems," *ASME J. of Applied Mechanics*, vol. 32, pp. 583–588, 1965.

[34] G. Strang and S. MacNamara, "Functions of difference matrices are toeplitz plus hankel," *SIAM Review*, vol. 56, no. 3, pp. 525–546, 2014.

[35] B. K.P. Horn and L. Wang, *Numerical simulations of inhomogeneous traffic flow under bilateral control*. [Online], Dec. 2018. Available: http://people.csail.mit.edu/bkph/TrafficFiles/inhomotraffic.html